In-situ SEM/EBSD Study of Deformation and Fracture Behaviour of Flake Cast Iron

Mattias Lundberg[1,*], Mattias Calmunger[1], Ru Lin Peng[1]

[1] Department of Management and Engineering, Linköping University SE-581 83 Linköping
*Corresponding author: mattias.lundberg@liu.se

Abstract Cast irons' position as an important engineering material is un-disputed. They are widely used in many important industrial applications such as the automotives and workshop machinery. Nevertheless, fracture mechanisms in cast irons are not fully understood. In this study the fracture path and non-linear elastic behaviour of a fully pearlitic flake cast iron under uniaxial tensile loading have been investigated in a Scanning Electron Microscope (SEM) equipped with an Electron Backscattering Diffraction (EBSD) detector. The tensile load was applied via a specially made sample stage. Under uniaxial tensile loading the graphite flakes act as notches or cracks and therefore the fracture process starts at one or many graphite tips. The crack can propagate in many different ways, at the graphite and matrix interface, through the graphite, at the interface between cementite and ferrite or through the pearlitic grains. At the point where the stress strain curve deviates from its linear path plastic deformation at graphite tips can be noticed. Interface cracking between graphite and the matrix also starts at this point.

Keywords in-situ SEM, deformation, fracture, flake cast iron, EBSD

1. Introduction

Flake cast iron exhibits brittle failure under tension loading. Due to its many graphite tips acting as notches or small cracks they are considered to be initiation points for cracks in the material. The common knowledge on how cracks propagates in flake cast irons is that the crack initiation point is one or several of the many graphite tips, from the tips the crack propagates along the graphite flakes in the graphite-matrix interface. At strains just before break down, the crack propagates through the matrix and connecting graphite tips.

In a work done by Diószegi at al [1] the crack path was found to be through eutectic cells and along the graphite flakes. Depending on cooling condition the main crack path varied so to propagate along dendrites.

The mechanisms explaining the non-linear stress-strain curve founded for flake cast irons involves a small plastic zone at graphite tips [2]. A typical stress-strain curve for a flake cast iron with σ_{UTS} of 290 MPa can be seen in Figure 3. As can be seen there is a small portion when the curve is straight linear; according to literature the explanation for this linear part is the atomic bonds and the interface forces between the graphite and the matrix [3, 4]. Plastic deformation at graphite tips and separation between graphite and matrix seems to be an excepted description what happens in the material when the stress-strain curve starts to deviate from its linear path during tensile loading [4].

An electron backscatter detector (EBSD) uses kikuchi patterns and a database to identify crystal structure and crystallographic orientation. Especially grain lattice orientation and grain size is commonly determined with this technique [5-10]. Texture analysis of metallic material using EBSD is a commonly usages of this technique [8, 10-11]. Strain variations in each grain near the machined surface give vital information on damages from machining processes [12]. From distribution and amount of low angle grain boundaries (LAGB) in the material, strain variations from external forces as well as from the solidification process can gathered. In a work done by Bjerkaas at al. on an AlMgSi alloy the benefits of this technique (EBSD) shows that grain lattice orientation during

tensile testing depends much on originally un-tested grain orientation, so different slip systems becomes active depending on grain orientation [6].

Several different research groups have performed tensile in-situ scanning electron microscope (SEM) investigations, studying microstructural changes and deformation and/or fracture mechanisms on different materials [6, 10, 13-15]. From their experiments one can conclude that in-situ SEM investigations can give very accurate information about microstructural changes due to external forces. Some of the recent works in this field have also performed EBSD to analyse the microstructural changes, e.g. grain orientation and grain reorientation, due to loading.

In this study the crack initiation point(s) and crack propagation in a grey cast iron where studied during axial loading in a SEM. Thanks to a specially designed stage mounted to the SEM, in-situ analysis of the crack initiation and its propagation as well as crystallographic changes were detected with EBSD and analysed. The microstructural features associated with different proportions of the stress-strain curve were investigated and explained.

2. Experimental details

The flake cast iron had a fully pearlitic matrix and the composition of the material used is listed in Table 1 below.

Table 1. Nominal composition of flake cast iron used

Element	C	Si	Mn	P	S	Cu	Cr	Mo	Fe
Wt %	3.1	1.8	0.65	<0.08	0.12	0.90	0.14	0.25	Bal.

The samples were cut out to a thickness of 1.0 mm from an as-cast cylinder head, using an electronic discharge wire to minimize the effects of surface hardening and residual stresses. On one side of the sample a notch was cut out with a total depth of 1.0 mm and a notch root radius of 0.25 mm. Both sides of the samples were carefully grinded and one side future prepared for EBSD analysis. On the rougher side of the sample a strain gauge were attached to enhance the accuracy of the actual loading when inside the SEM. Due to the brittleness of flake cast iron and the small elongation before rapture, some points on the stress strain curve in vacuum could then be conducted. Strain gauge signals were transmitted through pins on the stage specially designed for signal transmission from the vacuum chamber.

The samples were investigated at loadings of approximately 0 MPa, 50 MPa, 90 MPa, 140 MPa, 200 MPa and 250 MPa. EBSD mapping with a step size of 0.3 µm and SE images on each loading were performed in a Hitachi SU-70 FEG-SEM equipped with an OXFORD Electron Backscatter Diffraction system with HKL software. Due to contamination of the surface (carbon diffusion from the material when the electron beam hits the sample) from the EBSD analysis two different locations were used.

In all the figures the loading axis is in the horizontal plane, excluding Figure 3 and Figure 7.

3. Results

The un-tested material shows a great amount of LAGB, Figure 1c display the frequency distribution of LAGB and grain boundaries (GB). Revealing that LAGB of 2-3° is most common and that GB most commonly have angels around 30° and 60°. Figure 1b also reveals where the LAGB and GB are located; the most common LAGB is represented as red line and is randomly distributed in the microstructure. This resulted in two different LAGB intervals in this analysis to increase the detectability of LAGB changes. They are denoted as type I (2-6 °, red lines) and type II (6-12 °, green lines) LAGB respectively.

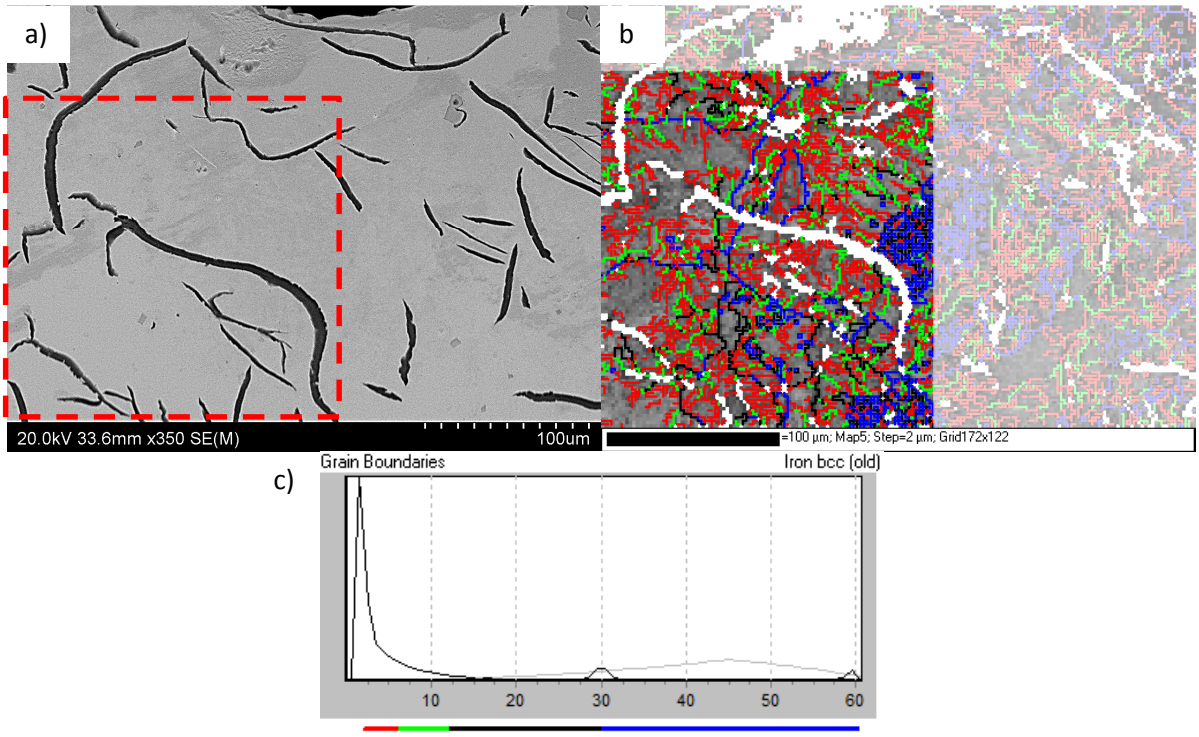

Figure 1. Display a) SE-picture with red marked EBSD-analysis area, b) EBSD-map showing band slope and the distribution of LAGB and grain boundaries (GB) and c) the grain boundary legend shows the colour of corresponding angle [°] and the frequency distribution of LAGB and GB. Zero solution is marked white.

In Figure 2 the LAGB distribution can be seen when a force corresponding to 200 MPa is applied. In Figure 2a graphite flakes have become larger due to internal cracking and matrix-graphite interface delamination, despite this the LAGB:s is unchanged.

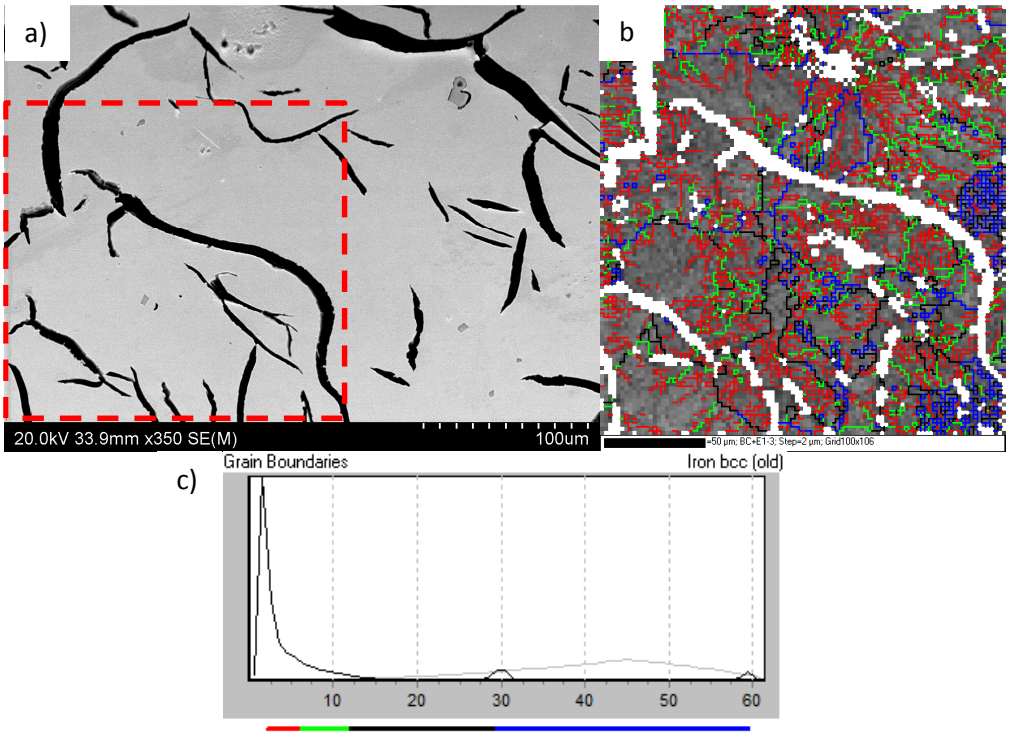

Figure 2. Display a) SE-picture with red dots marking the area of EBSD-analysis, b) EBSD-map showing band slope and the distribution of LAGB and grain boundaries (GB) and c) the grain boundary legend shows the colour of corresponding angle [°] and the frequency distribution of LAGB and GB. Zero solution is marked white.

The pure linear elastic part of a typical stress-strain curve for a flake graphite iron can related to the small tensile load that the graphite can withstand without microscopic yielding [16, 17] and the atomic forces. In this region the SE images did not revile any changes in the microstructure in neither the matrix nor the graphite. Also the EBSD mapping looks the same as in the un-stressed case, no statistical significant changes were found.

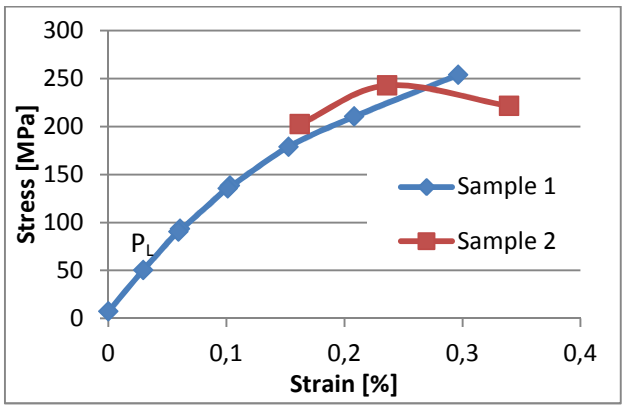

Figure 3. Obtained stress-strain curve from the experiment.

What then can be seen in SE-images, see Figure 2, when the applied load is slightly more than the critical value $P_{L;}$ (were the stress-strain curve starts to deviate from its linear path) the flaky graphite tends to open in the middle and a void appears inside. This phenomenon can be seen and detected in graphite orientated both perpendicular and parallel to the loading axis at loading levels above P_L ,

see Figure 3. At this stage the changes in the matrix is still too small to be detected with the set-up used.

When increasing the load, ($P>P_L$) the interface between the flaky graphite and the matrix starts to separate at several places in the material, mostly graphite flakes oriented perpendicular to the load shows this phenomenon. Still the cracks/voids earlier founded inside the flaky graphite opens more independent of the graphite's orientation, but the degree of opening is more evidence in graphite perpendicular to the load axis. The pearlitic matrix also starts to undergo microplasticity at several graphite tips, the matrix undergo local plastically deformation which can be seen in Figure 4 and Figure 5.

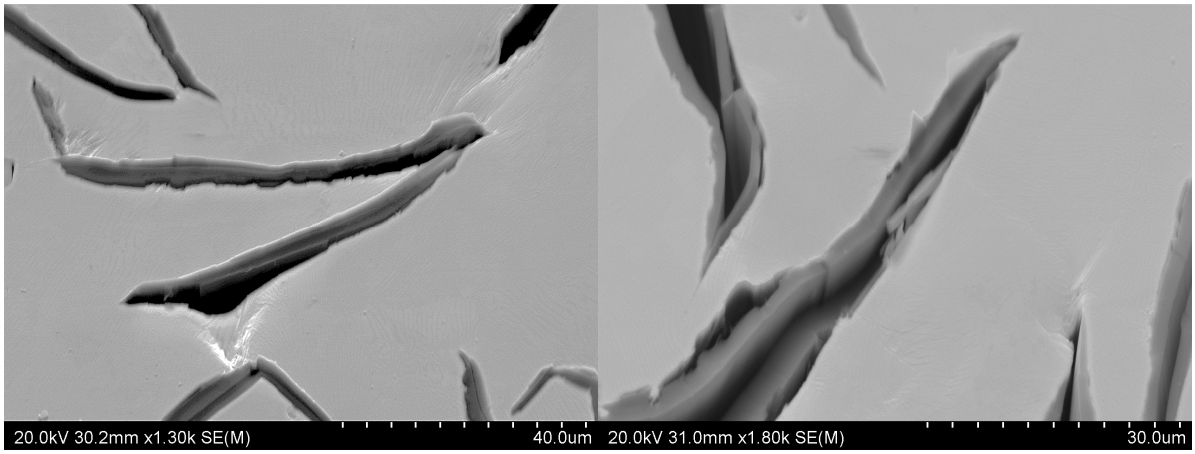

Figure 4. Plastic deformation at graphite tips and a bulge is evidence in the left picture. To the right multiple cracking with crack path both inside the graphite and at the graphite-matrix interface can be seen.

The delamination of the graphite-matrix interface is easy to identify and when increasing the load even more, above 200 MPa, small bulges in the separated graphite-matrix interface is evidence of the weakest pearlite, see Figure 4. Here at these bulges the matrix limited plasticity results in a crack path when the load is increased even more, local necking in the matrix.

At loads above $\sigma_{ys0.2\%}$ the crack also finds its way through the matrix in the ferrite-cementite interface as can be seen in Figure 5 below.

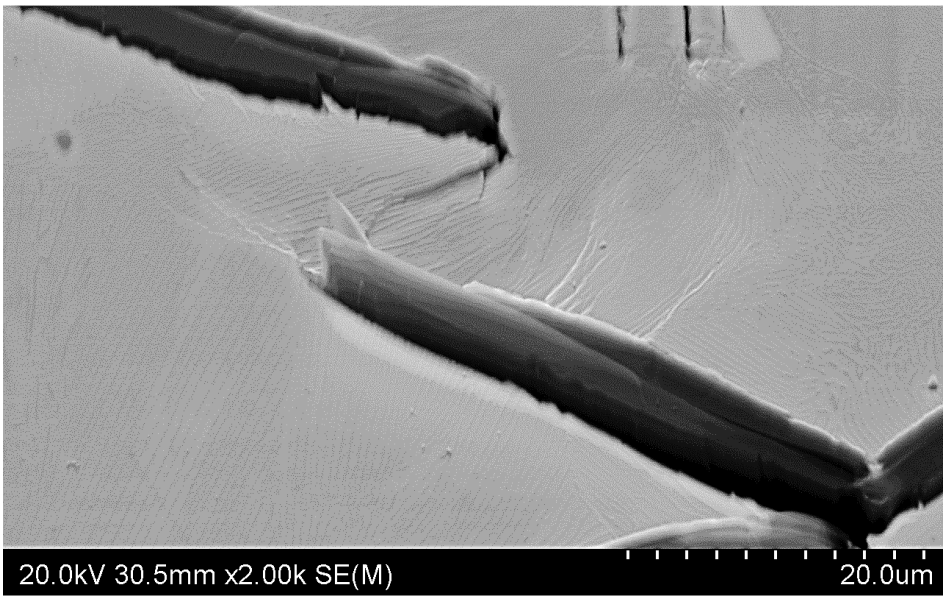

Figure 5. Cracking in the ferrite-cementite interface between two graphite tips.

At stresses above $\sigma_{ys0.2\%}$ the phenomenon of multiple cracking is also evident in the material, showing the complexity of the fracture behaviour of the material. In Figure 6 below this phenomenon can easily be seen in the left picture. The right picture is zoomed out from the left showing obviously multiple cracking.

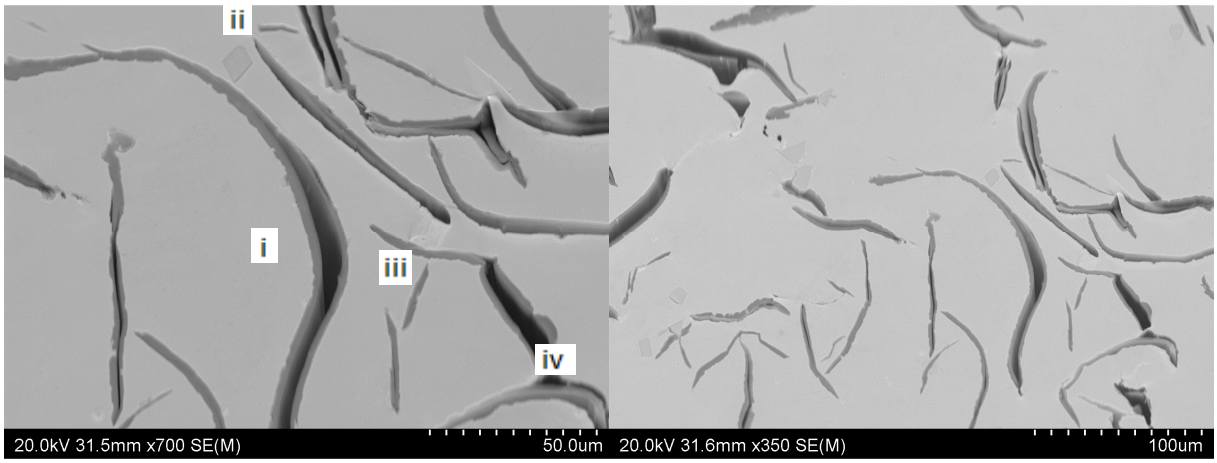

Figure 6. Showing voids inside graphite flakes (i), delamination of the graphite-matrix interface (ii), plastic deformation at graphite tips (iii) and a bulge (iv).

Fractorgraphy revealed that both ductile-like and cleavage-like fracture is present in flake cast iron. Near the notch almost all pearlite grains showed evidence of ductile crack surface, whereas the opposite side of the sample showed mainly river-pattern in the cracked pearlite associated with cleavage fracture. In Figure 7 below both these features can be seen along with a part of a graphite flake.

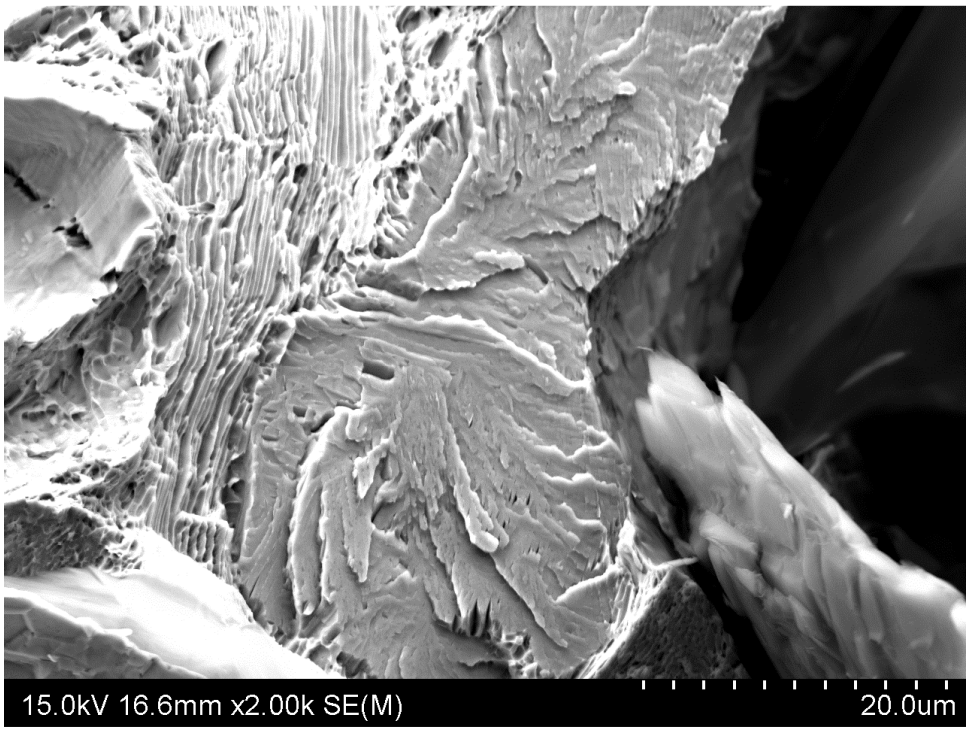

Figure 7. Fracture surface showing features associated with both ductile and brittle fracture in the pearlite matrix. On the right side a part of a graphite flake is seen.

4. Discussion

Even though pearlitic flake cast iron is widely used and is an important engineering material the knowledge on its fracture behaviour and the deformation due to axial loading is still very limited. One of the main goals with this research was to gain deeper knowledge on the deformation and fracture behaviour of a pearlitic flake cast iron. The use of the special designed stage in the SEM together with EBSD analysis can give a unique insight in the deformation and fracture behaviour of the material studied. In this study the amount of pre-existing LAGB's made the analysis of their changes due to loading very difficult and no clear effects where shown. The great amount of LAGB's detected is an effect of the solidification process and the material used had not been stress-relived. The heat treatment should decrease the amount of LAGB's once the internal thermal residual stresses from the solidification process minimizes. One aim with this study was to investigate the LAGB changes and the grain orientation due to axial loading and from these results no changes were detected.

The deformation of a flake cast iron under axial loading can be divided into several different main events. First deformation detected in the material was the development of voids inside graphite flakes. This material deformation was detected at loads as low as 50 MPa and the strength of the weakest slip plane in the graphite is approximately 40 Mpa which then makes the fact that it separates at 50 Mpa very understandable. With compressive residual stresses presence at the surface this deformation would not be seen at this load-level and thanks to careful polishing this effect could be discovered. Interesting to see is that when increasing the load these voids can be found in graphite flakes independent of its orientation to the load axis. Delamination of the graphite-matrix interface was the second kind of deformation detected in the material. This deformation requires slightly more applied load and a suggested explanation for this is that the interface forces between the two phases is just greater than the weakest slip plane in the graphite. By looking at the stress strain curve seen in Figure 3 one can see that curve deviates from its linear path at stresses between 50 and 90 Mpa and it is proposed by the authors that this is an effect of both the delamination of the graphite-matrix interface and the presence of voids inside the graphite flakes. These effects are also responsible in the change of Young´s modulus as seen in for flake cast iron subjected to cyclic loading, less elastic deformation is possible for this multi-phased material. Plastic deformation at graphite tips was the third permanent deformation detected in the material. Loads generating stresses in the magnitude of 140 Mpa and more results in plastic deformation at graphite tips. With increasing load the size of the plastic zone is increased and also amount of plastic deformation around graphite tips increases with increasing load. This is expected to be seen but not that the sizes of voids inside graphite flakes to decrease for those voids lying a bit away from the real crack path. Obviously some kind of stress relaxation occurs in the material when the pearlite starts to hardens due to the plastic deformation at the graphite tips. The last type of deformation detected was the development of bulges just before rapture, as a consequence of stress concentrations at the graphite. When study the final fracture it was then evident that the crack path had been via these bulges. The plastic deformation at these bulges is severe and a phenomenon of local necking is present.

Fracture behaviour becomes more and more complex as the applied load increases and several distinct features acting simultaneously resulting in final failure. The graphite tips acts as notches and clearly the plastic deformation at the tips indicates where the crack later will propagate. Due to multiple cracking not every graphite flake with local plastic deformation at the tip will be a part of the final cracking. Fractography reviled a ductile fracture where the bulges earlier had been detected leading to the conclusion that severe plastic deformation at the tips results in the ductile-like fracture found in the material.

Not every graphite flake that opens inside contributes to the final crack but once they have opened it affects the mechanical properties of the cast iron. It has been identified in this investigation that the first fracture observed in the material actually occurs inside the graphite flakes followed by delamination of the graphite-matrix interface. The non-linear elastic behaviour and the decrease in Young´s modulus observed in flake cast iron is proposed by the authors to a result of these two permanent deformation phenomenon´s in the material.

5. Conclusions

The fracture behaviour of flake cast iron can be summarized in a few steps of main events. The first noticeable microstructural feature due to the axial loading is the opening of graphite. Graphite flakes opens inside the flakes and this feature can be found in graphite flakes independent of its orientation to the applied load. As a second important and noticeable event is the delamination of the graphite-matrix interface. Parallel to this event one can see that the graphite that had opened inside opens even more. The third crack feature is the local plasticity at graphite tips laying perpendicular to the loading. Fourth and last important feature is the bulge of the matrix at the delaminated interface, where the crack later will propagate. Some of the graphite with an opening inside had also generated a delamination of the graphite-matrix interface. Development of bulges start once the plastic deformation at graphite tips is evidence but stresses close to and above $\sigma_{ys0.2\%}$ is needed to clarifying that a bulge is developed and not just local plastic deformation. At applied loadings just before rapture the fracture behaviour of flake cast iron results in multiple cracking, which makes it possible for the main crack to “jump” relatively large distances due to the network of flaky graphite. The weakest points in the sample will then link together which results in a rough topography of the fracture surface. As a final occurrence of fracture behaviour in flake cast iron subjected to axial loading the crack propagates in one of the following alternatives:

- Through the opening inside the graphite.
- Through the delaminated interface.
- Via the closest distance between graphite tips where the local plastic deformation results in a ductile-like fracture appearance.
- At the pearlitic grain boundaries leaving a ductile-like fracture.
- Straightforward through the matrix resulting in a cleavage fracture.
- Along the ferrite-cementite interface giving cleavage fracture.

Grain orientation and changes of LAGB’s in flake cast iron due to axial loading is very small, if existing, the relative fine step-size used could not show any differences. Fractography give instant insight why the crack propagated to the right in Figure 1 and not on the left side as large graphite flakes where located just below the surface to the right and not to the left. Analyse of the fractured surface revealed both ductile and cleavage fracture and an increase in fracture topology where multiple cracks was easily detected.

Acknowledgment

The authors would like to thank Maqsood Ahmad from Volvo Powertrain for providing the material. Agora Materiae graduated school at Linköping University.

References

[1] A. Diószegi, V. Fourlakidis, I.L. Svensson, Fracture Mechanics of Gray Cast Iron, Material Science Forum, 649 (2010) 517-522.
[2] L. Haenny, G. Zambelli, Strain Mechanisms in Grey Cast Iron, Engineering Fracture Mechanics, 18 (1983) 377-387.
[3] H.T. Angus, Cast Iron, Butterworth, London, 1976.

[4] T. Sjögren, Influence of the Graphite Phase on Elastic and Plastic Deformation Behaviour of Cast Irons, Linköping Studies in Science and Technology Dissertations No. 1080, Linköping.
[5] A.J. Schwartz, Electron Backscattering Diffraction in Material Science, Springer Science + Business Media, New York, 2009.
[6] H. Bjerkaas, S.K. Fjeldbo, H.J. Roven, J. Hjelen, R. Chiron, T. Furu, Study of Microstructure and Texture Evolution using In-situ EBSD Investigations and SE Imaging in SEM, Material Science Forum, 519-521 (2006) 809-814.
[7] S. Ifergane, Z. Barkay, O. Beeri, N. Eliaz, Study of Fracture Evolution in Copper Sheets by In-situ Tensile Test and EBSD Analysis, Journal of Material Science, 45 (2010) 6345-6352.
[8] M.F. de Campos, L.C. Rolim Lopes, P. Magina, F.C. Lee Tavares, C.T. Kunioshi, H. Goldenstein, Texture and Microtexture Studies in Different Types of Cast Irons, Material Science and Engineering A, 398 (2005) 164-170.
[9] M. Kamaya, Assessment of Local Deformation Using EBSD: Quantification of Local Damage at Grain Boundaries, Materials Characterization, 66 (2012) 56-67.
[10] M. Ferry, W. Xu, Microstructural and Crystallographic Features of Ausferrite in As-cast Gray Iron, Materials Characterization, 53 (2004) 43-49.
[11] G. Rivera, P.R. Calvillo, R. Boeri, Y. Houbaert, J. Sikora, Examination of the Solidification of Spheroidal and Flake Graphite Cast Irons using DAAS and EBSD, Materials Characterization, 59 (2008) 1342-1348.
[12] R. Lin Peng, Y.D. Wang, G. Chai, N. Jia, G. Wang, S. Johansson, On the Development of Grain-orientation-dependent and Inter-phase Stresses in a Super Duplex Stainless Steel Under Uniaxial Loading, Material Science Forum, 524-525 (2006) 917-922.
[13] V. Di Cocco, F. Iacoviello, M. Cavallini, Damaging Micromechanisms Characterization of a Ferritic Ductile Cast Iron, Engineering Fracture Mechanics, 77 (2010) 2016-2023.
[14] F. Iacoviello, O. Di Bartolomeo, V. Di Cocco, V. Piacente, Damaging Micromechanisms in Ferritic-Pearlitic Ductile Cast Irons, Materials Science and Engineering A, 478 (2008) 181-186.
[15] A. Ghahremaninezhad, K. Ravi-Chander, Deformation and Failure in Nodular Cast Iron, Acta Materialia, 60 (2012) 2359-2368.
[16] J.R. Dryden, G.R. Purdy, The Effect of Graphite on the Mechanical Properties of Cast Irons, Acta Metallurgica, 37 (1989) 1999-2006.
[17] D.D. Double, A. Hellawell, Defects in Eutectic Flake Graphite, Acta Metallurgica, 19 (1971) 1303-1306.